ELSEVIER

Materials Science and Engineering A 431 (2006) 196–200

MATERIALS SCIENCE & ENGINEERING A

www.elsevier.com/locate/msea

First-principles calculations and phenomenological modeling of lattice misfit in Ni-base superalloys

Tao Wang *, Long-Qing Chen, Zi-Kui Liu

Department of Materials Science and Engineering, The Pennsylvania State University, University Park, PA 16802, United States

Received 29 September 2005; received in revised form 19 May 2006; accepted 31 May 2006

Abstract

An integrated computational approach is proposed for evaluating the lattice misfit between γ and γ' in Ni-base superalloys by combining first-principles calculations, existing experimental data and phenomenological modeling. In particular, the lattice misfits in Ni–Al and Ni–Al–Mo alloys were studied. This approach is validated by comparing the calculated lattice misfit with available experimental measurements as well as by comparing the predicted γ' precipitate morphologies from phase-field simulations with experimental observations.

Keywords: First-principles calculation; Lattice misfit; Ni-base superalloys; Phase-field simulation

1. Introduction

The $L1_2$ ordered precipitate γ' coherently embedded in the fcc matrix γ is the primary strengthening phase in Ni-base superalloy. Its morphology plays an important role in high-temperature properties of nickel-base superalloys. It has been shown that one of the critical factors that control the morphology of coherent γ' precipitates is the magnitude and sign of the stress-free lattice misfit between γ and γ'. The lattice misfit is calculated from the stress-free lattice parameters of the γ and γ' phases, which are typically measured by X-ray diffraction method (XRD) [1] or convergent beam electron diffraction method (CBED) [2]. The results are very sensitive to the details of alloy processing [3], and the incoherent and equilibrium conditions must be satisfied for a measurement in a multi-phase mixture. Consequently, the results of lattice misfit from different reports are usually very scattered, especially for nickel-base superalloys where the lattice parameters of γ and γ' are close to each other. The problem of scattered experimental data is even more serious for multi-component systems. The main objective of this work is to develop an integrated computational approach by combining first-principles calculations and phenomenological modeling. In particular, we applied this approach to obtaining the lattice misfit in both Ni–Al binary and Ni–Al–Mo ternary alloys as Mo is one of most common species in Ni-base superalloys. The lattice misfit, is then used in our phase-field simulations to predict the morphology of γ' precipitates as a function of Mo composition.

2. Methodology

2.1. Lattice parameters of pure metals and ordered compounds

In the last decade, first-principles calculations have been extensively used to obtain the formation energies, band structures and lattice parameters of pure metals and compounds, which are particularly valuable for cases where experimental data are not available. In the present work, the first-principle calculations of lattice parameters in the Ni-superalloy system are performed using the Vienna ab initio simulation package VASP 4.6 [4]. The total energy of a system is minimized with respect to both the volume and shape of a computational cell and the atom positions within the cell. In the present calculations, the ultrasoft pseudopotentials and the generalized gradient approximation (GGA) [5] are adopted. It has been generally known that GGA partially corrects the overbinding problem of the local density approximation (LDA) [6], and thus improves the predictions for the equilibrium volumes [7,8]. The set of k points is chosen according to the size of the computational cell, and a $4 \times 4 \times 4$ k-point mesh is selected for the supercell used in the present calculations. The energy cutoff is determined by the choice of "high accuracy" in VASP, and set to be 314 eV in calculations

* Corresponding author. Tel.: +1 814 863 9957; fax: +1 814 865 2917.
E-mail address: taowang@psu.edu (T. Wang).

0921-5093/$ – see front matter © 2006 Elsevier B.V. All rights reserved.
doi:10.1016/j.msea.2006.05.152

Table 1
Lattice parameters of ordered and disordered phases

	a_0 (Å)		$\Delta a_T = bT + cT^2$ (Å)	
	Calculated (0 K)	Experimental (298 K) [3]	b (Å/K) [11]	c (Å/K^2) [11]
γ(Ni)	3.532	3.523	5.741×10^{-5}	-1.010×10^{-9}
γ′(Ni_3Al)	3.573	3.552–3.589	6.162×10^{-5}	-1.132×10^{-8}

for Ni–Al–Mo alloys. For a detailed description of the technical features and the computational procedure of the VASP calculations we refer to the VASP's manual [9]. The calculated lattice parameters of pure Ni and Ni_3Al compound (a_0) are compared with the experimental data in Table 1.

To predict the lattice parameters at finite temperatures, thermal expansion information is required. It can be determined experimentally (e.g. diffraction measurements) or theoretically (e.g. first-principles linear-response theory) [10]. However, there is still about a 10% uncertainty in the thermal expansion coefficients obtained from the theoretical calculations due to various assumptions and approximations [10]. Such an uncertainty can lead to an error of ∼0.0035 in the misfit between γ and γ′ in nickel-base superalloys at 1000 K. This error is significant since the measured lattice misfit in Ni–Al binary alloys is only about 0.004 at 1000 K [3]. Therefore, we still relied on experimental data for the thermal expansion coefficients of γ and γ′. In particular, we used those values reported by Kamara et al. [11] who described the temperature effect (Δa_T) by a quadratic function of temperature:

$$\Delta a_T = bT + cT^2 \quad (1)$$

where b and c are constants (see Table 1).

2.2. Effect of chemical disordering

In the Ni–Al binary system, γ′ has an ordered fcc structure with two sublattices. One sublattice is made up of face-centered sites occupied mostly by Ni atoms (Ni site), and the other sublattice consists of fcc corner sites occupied mostly by Al atoms (Al site). The degree of chemical order in γ′ decreases with temperature increasing by mean of anti-sites, i.e. Ni atoms go to Al site and Al atoms go to Ni site. The off-stoichiometry of γ′ is also realized by anti-site atoms. In multi-component systems, various solute species are also expected to have random distributions over the two sublattices although the amounts of a given species are typically different in the two sublattices. These chemical disorders (due to the changes in composition and temperature) lead to the changes in the lattice parameters. If these types of chemical disorders are relatively small, we can approximate their effect on lattice parameter (Δa_C) using a linear combination:

$$\Delta a_C = \sum_s \sum_i k_i^s y_i^s \quad (2)$$

where s indicates different sublattices, y_i^s is the atomic fraction of element i in sublattice s, and k_i^s is the coefficient representing the effect of i in the s sublattice.

γ has a disordered fcc structure, where both sites are equivalent, and all atoms are in random mixing. We can still use Eq. (2) to describe the composition effect on the lattice parameter change of γ, and the site fractions y_i here are same for all sublattices and equal to x_i, the atomic fractions in the γ phase.

In this work, we determine k_i^s by using first-principles supercell calculations. Each supercell contains one solute or anti-site in a given sublattice. k_i^s is then calculated using the following equation:

$$k_i^s = N(a_i - a_0) \quad (3)$$

where a_0 presents the calculated lattice parameter for pure Ni or the completely ordered cell, a_i is the calculated lattice parameter of the supercell containing one i atom in sublattice s, and N is the total number of atoms in the supercell. In all calculations, the total number of atoms is 108. The determined linear coefficients of solute or anti-site elements are presented in Table 2.

2.3. Lattice misfit

The dependences of lattice parameters of $\gamma(a_\gamma)$ and $\gamma'(a_{\gamma'})$ on temperature and compositions are described by the following equation:

$$a_{\gamma,\gamma'} = a_0 + \Delta a_T + \Delta a_C = a_0 + bT + cT^2 + \sum_s \sum_i k_i^s y_i^s \quad (4)$$

For any given temperature T and composition x_i, the site fractions in each phase can be obtained from the thermodynamic databases by Dupin et al. [12] for Ni–Al and Zhou et al. [13] for Ni–Al–Mo. The lattice misfit (δ) between γ and γ′ can then be calculated from its definition, i.e.:

$$\delta = \frac{a_{\gamma'} - a_\gamma}{a_\gamma} \quad (5)$$

Table 2
Linear coefficients of solute or anti-site elements in the γ and γ′ phases (in Å/at.%)

i	γ	γ′	
	k_i^I	k_i^I	k_i^{II}
Ni	0	0	−0.044
Al	0.159	1.077	0
Mo	0.405	0.819	0.042

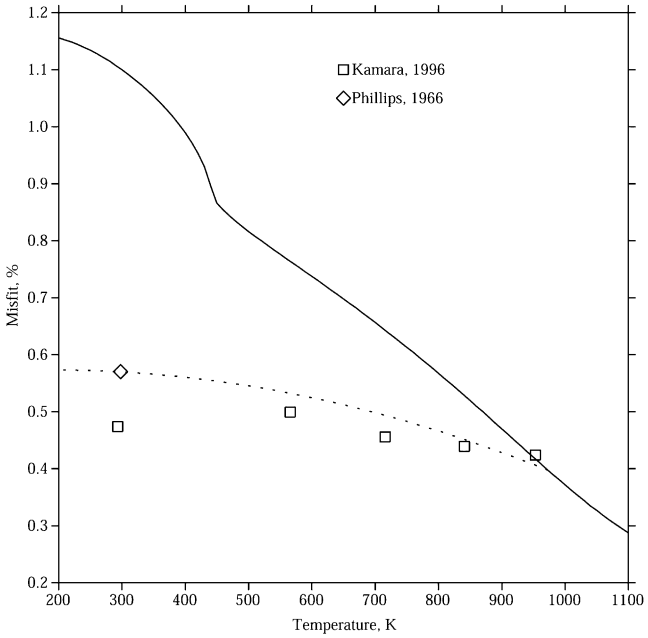

Fig. 1. Lattice misfit between γ and γ′ in the Ni–Al binary system. (Curves present calculated results, and symbols are reported experimental values from literature: (□) [11] and (◇) [14]).

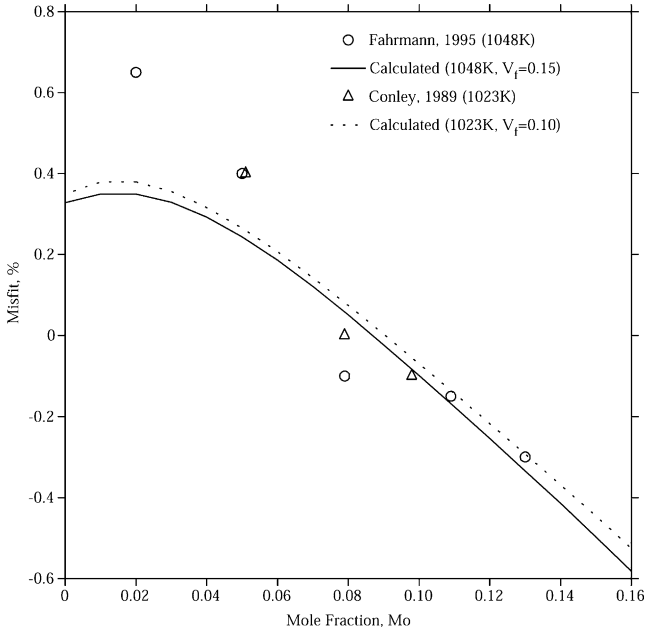

Fig. 2. Lattice misfit γ and γ′ in Ni–Al–Mo ternary system. (Curves present calculated results, and symbols are reported values from literature: (◯) [16] and (△) [15]).

3. Results and discussions

3.1. Ni–Al binary system

Using the approach described above, the lattice misfits between the γ and γ′ phases in Ni–Al binary systems are predicted and plotted in Fig. 1. The misfits shown by the solid curve were obtained by assuming the two phases are at thermodynamic equilibrium at each temperature. The symbols represent the experimentally determined lattice misfits [11,14]. Clearly, the agreement between the solid curve and the experimental data points are poor. However, such a discrepancy can be easily explained. The misfits in this work were evaluated assuming equilibrium conditions at all temperatures, while the experimental measurements at different temperatures were performed on samples quenched from 973 K. Therefore, the phases in the samples were expected to maintain their equilibrium compositions at 973 K [3]. To test this hypothesis, we fixed the site fractions y_i^s as the equilibrium values corresponding to 973 K, and then calculated the lattice misfits between the γ and γ′ phases in Ni–Al binary system at different temperatures. The results are presented by the dotted line in Fig. 1. Indeed an excellent agreement is achieved by comparing the dotted line and the experimental data points.

3.2. Ni–Al–Mo ternary system

Conley et al. [15] measured the room temperature lattice parameters of γ and γ′ in three Ni–Al–Mo alloys using precision Debye–Scherrer powder X-ray method. The volume fractions of γ′, V_f, are around 0.10. The sample were quenched from 1023 K, and the lattice misfits at 1023 K were then evaluated assuming constant thermal expansion coefficients for γ and γ′. Fahrmann et al. [16] determined the lattice misfits of five Ni–Al–Mo alloys at 1048 K using high-temperature X-ray diffraction. The volume fractions of γ′ of alloys are between 0.10 and 0.20. Since the measurements were performed on coherent microstructures, they artificially increased the values for the lattice misfit by a factor of 1.5 to approximate the coherency strain effect [16].

The dependence of the predicted lattice misfits on alloy composition in Ni–Al–Mo is shown in Fig. 2. In general, with the increase in Mo concentration, the lattice misfit decreases and changes sign from positive to negative. This trend agrees with the above-mentioned experimental measurements [15,16]. As shown in Fig. 2, the agreement between experimental data (symbols) and our calculations (curves) are generally good except for the alloy with the lowest Mo concentration (Ni–12.5 at.% Al–2.0 at.% Mo) from Fahrmann et al. [16]. First, since the Mo concentration is very small in this alloy, its lattice misfit should be close to that in Ni–Al binary alloys at the same temperature, i.e. 0.004 (see Fig. 1). Second, Fahrmann et al. [16] reported that the microstructure of this alloy was semicoherent instead of coherent, but they multiplied the same factor of 1.5 to estimate the corresponding stress-free misfit, which probably overestimated the stress-free misfit.

3.3. Phase-field simulation of γ′ precipitate morphology

Using the predicted lattice misfit, phase-field simulations were carried out to predict the γ′ precipitate morphology. A comparison between the predicted and experimentally observed morphology provides another indirect evidence on the accuracies of the prediction of lattice misfit data. In the phase-field method, a microstructure is described by a set of physical or artificial fields, and its temporal and spatial evolution is governed by

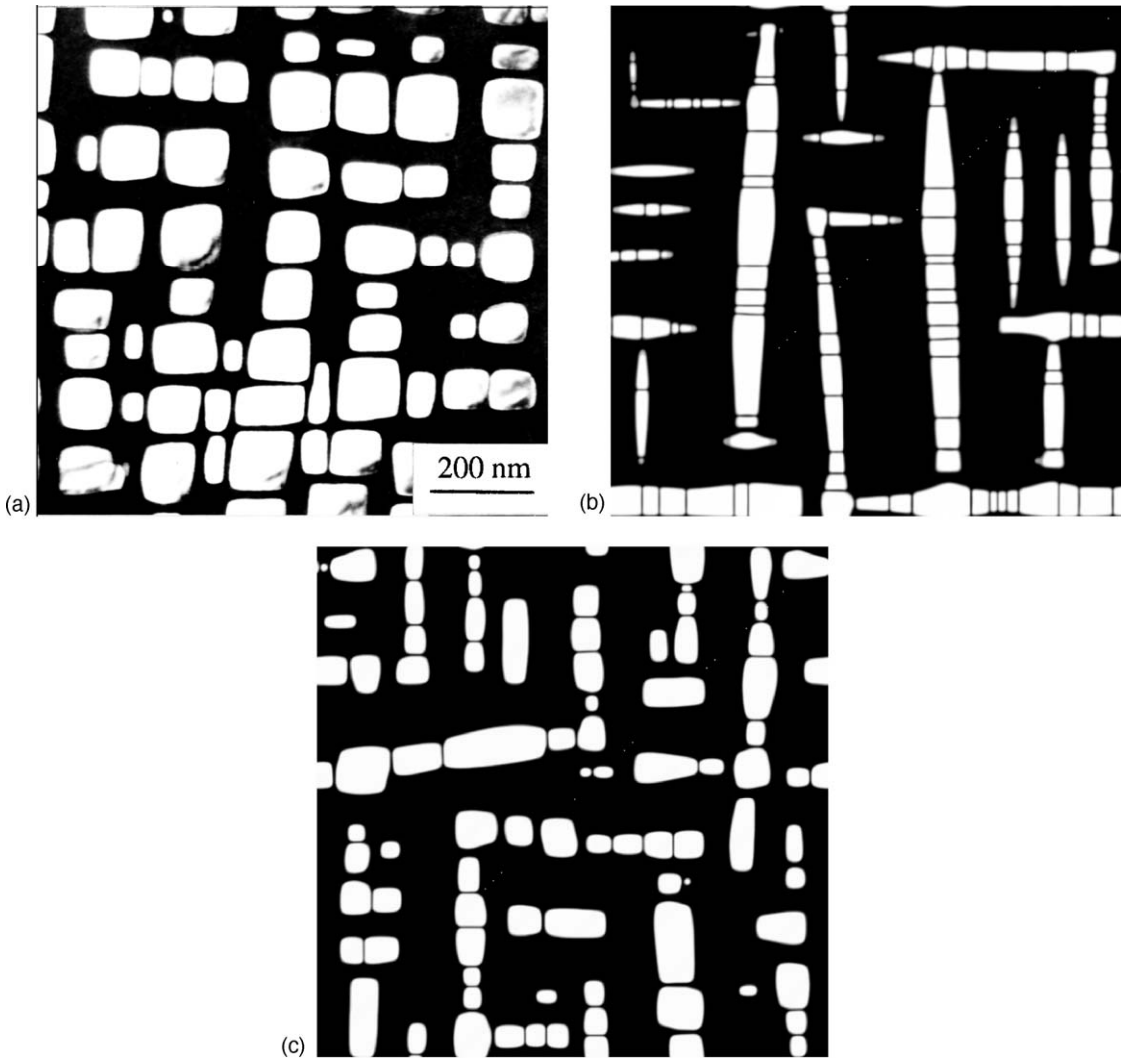

Fig. 3. Comparison of precipitate morphologies, obtained by experiments [16] (a) and 2D phase-field simulations (b and c) in a Ni–12.5 at.% Al–2.0 at.% Mo alloy aged at 1048 K for 67 h: (b) $\delta = 0.0065$ and (c) $\delta = 0.0035$.

a set of mathematical equations of the fields [17]. With reliable input data (properties of the system, e.g. thermodynamic driving force, atomic mobility, lattice misfit and elastic constant), the microstructure evolution and coarsening kinetics can be predicted quantitatively. The simulation details can be found in Ref. [17].

We investigated the γ' precipitate morphologies in an alloy with composition Ni–12.5 at.% Al–2.0 at.% Mo using 2D phase-field simulations. Two sets of different misfit data (0.0065 from Fahrmann et al. [16] and 0.0035 from the present work) were used. The precipitate morphologies from experimental observation (a) and phase-field simulations (b and c) are shown in Fig. 3. The precipitate sizes from both simulations are somewhat smaller than that from experiments. One of the reasons could be due to the 2D nature of simulations since the coarsening in 2D is slower than 3D because of the reduced curvature. However, it is quite evident that the morphology using $\delta = 0.0065$ (Fig. 3(b)) is quite different from that observed experimentally. The lenticular shape and strong alignments are caused by large elastic stresses, indicating an overestimated misfit. On the other hand, the particle shape in Fig. 3(c) obtained using $\delta = 0.0035$ is very similar to the experimental observation. This provides another indirect evidence that the predicted misfit in this work is reasonable.

4. Summary

An integrated computational approach is proposed for evaluating the lattice misfit between γ and γ' in Ni-base alloys. It combines the first-principles calculations of lattice parameters at 0 K, experimental data on thermal expansion coefficients, and phenomenological modeling. It was applied to the Ni–Al binary and the Ni–Al–Mo ternary systems. A comparison between evaluated lattice mismatch and experimental measurements shows good agreement in both its temperature and composition dependences. Using the calculated lattice misfit, the precipitate morphology of a Ni–Al–Mo alloy was predicted using a phase-field simulation and is shown to agree well with experimental observation.

Acknowledgments

This work is funded by the National Science Foundation (NSF) through grant DMR-0205232. First-principles calculations were carried out on the LION clusters at the Pennsylvania State University supported in part by the NSF grants (DMR-9983532, DMR-0122638, and DMR-0205232) and in part by the Materials Simulation Center and the Graduate Education and Research Services at the Pennsylvania State University. The authors also want to thank Dr. Michael G. Fahrmann for providing the original TEM micrographs.

References

[1] U. Bruckner, A. Epishin, T. Link, K. Dressel, Mater. Sci. Eng. A 247 (1998) 23–31.
[2] R. Volkl, U. Glatzel, M. Feller-Kniepmeier, Acta Mater. 46 (1998) 4395–4404.
[3] T. Wang, J.Z. Zhu, R.A. Mackay, L.Q. Chen, Z.K. Liu, Metall. Mater. Trans. A 35A (2004) 2313–2321.
[4] G. Kresse, J. Hafner, Phys. Rev. B 48 (1993) 13115–13118.
[5] J.P. Perdew, in: P. Ziesche, H. Eschrig (Eds.), Electronic Structure of Solids, Akademie Verlag, Berlin, 1991.
[6] R.O. Jones, O. Gunnarsson, Rev. Mod. Phys. 61 (1989) 689.
[7] A. Lindbaum, J. Hafner, E. Gratz, S. Heathman, J. Phys.: Condens. Mater. 10 (1998) 2933–2945.
[8] A. Lindbaum, J. Hafner, E. Gratz, J. Phys.: Condens. Mater. 11 (1999) 1177–1187.
[9] G. Kresse, J. Furthmuller, VASP the GUIDE, http://cms.mpi.univie.ac.at/vasp/vasp/vasp.html.
[10] Y. Wang, Z.K. Liu, L.Q. Chen, Acta Mater. 52 (2004) 2665–2671.
[11] A.B. Kamara, A.J. Ardell, C.N.J. Wagner, Metall. Mater. Trans. A 27 (1996) 2888–2896.
[12] N. Dupin, I. Ansara, B. Sundman, Calphad 25 (2001) 279–298.
[13] S.H. Zhou, Y. Wang, J.Z. Zhu, T. Wang, L.Q. Chen, R.A. MacKay, Z.K. Liu, Superalloys (2004) 969–975.
[14] V.A. Phillips, Acta Metall. Mater. 14 (1966) 1533–1547.
[15] J.G. Conley, M.E. Fine, J.R. Weertman, Acta Metall. Mater. 37 (1989) 1251–1263.
[16] M. Fahrmann, P. Fratzl, O. Paris, E. Fahrmann, W.C. Johnson, Acta Metall. Mater. 43 (1995) 1007–1022.
[17] J.Z. Zhu, T. Wang, A.J. Ardell, S.H. Zhou, Z.K. Liu, L.Q. Chen, Acta Mater. 52 (2004) 2837–2845.